Neoplasia • Vol. 9, No. 11, November 2007, pp. 970–978

www.neoplasia.com

Hypomethylation and Aberrant Expression of the Glioma Pathogenesis–Related 1 Gene in Wilms Tumors

Laxmi Chilukamarri[*,1], *Anne L. Hancock*[*,1], *Sally Malik*[*,1], *Joanna Zabkiewicz**, *Jenny A. Baker**, *Alexander Greenhough*[†], *Anthony R. Dallosso**, *Tim Hui-Ming Huang*[‡], *Brigitte Royer-Pokora*[§], *Keith W. Brown** *and Karim Malik*[*,1]

*Cancer and Leukaemia in Childhood, Sargent Research Unit, Department of Cellular and Molecular Medicine, School of Medical Sciences, University of Bristol, University Walk, Bristol BS8 1TD, UK; [†]Cancer Research UK, Colorectal Tumor Biology Group, Department of Cellular and Molecular Medicine, School of Medical Sciences, University of Bristol, University Walk, Bristol BS8 1TD, UK; [‡]Department of Molecular Virology, Immunology and Medical Genetics – Human Cancer Genetics, 656 Medical Research Facility, 420 W 12th Ave, Columbus, OH 43210, USA; [§]Institut für Humangenetik und Anthropologie, Heinrich-Heine Universität, Postfach 101007, Düsseldorf D40001, Germany

Abstract

Wilms tumors (WTs) have a complex etiology, displaying genetic and epigenetic changes, including loss of imprinting (LOI) and tumor suppressor gene silencing. To identify new regions of epigenetic perturbation in WTs, we screened kidney and tumor DNA using CpG island (CGI) tags associated with cancer-specific DNA methylation changes. One such tag corresponded to a paralog of the glioma pathogenesis–related 1/related to testis-specific, vespid, and pathogenesis proteins 1 (*GLIPR1/RTVP-1*) gene, previously reported to be a tumor-suppressor gene silenced by hypermethylation in prostate cancer. Here we report methylation analysis of the *GLIPR1/RTVP-1* gene in WTs and normal fetal and pediatric kidneys. Hypomethylation of the *GLIPR1/RTVP-1* 5′-region in WTs relative to normal tissue is observed in 21/24 (87.5%) of WTs analyzed. Quantitative analysis of *GLIPR1/RTVP-1* expression in 24 WTs showed elevated transcript levels in 16/24 WTs (67%), with 12 WTs displaying in excess of 20-fold overexpression relative to fetal kidney (FK) control samples. Immunohistochemical analysis of FK and WT corroborates the RNA expression data and reveals high GLIPR1/RTVP-1 in WT blastemal cells together with variable levels in stromal and epithelial components. Hypomethylation is also evident in the WT precursor lesions and nephrogenic rests (NRs), supporting a role for *GLIPR1/RTVP-1* deregulation early in Wilms tumorigenesis. Our data show that, in addition to gene dosage changes arising from LOI and hypermethylation-induced gene silencing, gene activation resulting from hypomethylation is also prevalent in WTs.

Neoplasia (2007) **9,** 970–978

Keywords: Wilms tumor, epigenetics, hypomethylation, *GLIPR1/RTVP-1*, overexpression.

Introduction

Wilms tumor (WT) is the most common solid tumor of childhood and represents a paradigm for tumorigenesis resulting from disrupted development [1]. Germline defects of chromosome 11p13 in Wilms tumor aniridia genitourinary abnormalities, and mental retardation (WAGR) signposted the identification of the tumor-suppressor gene *WT1* at this locus [2,3], which has subsequently been shown to have loss of function mutations in 5% to 10% of sporadic WTs [4]. More recently, a gene on chromosome Xq11, referred to as *WTX*, has been shown to be inactivated in about a third of WTs [5], but for a large proportion of WTs the etiology is undefined.

In addition to genetic events, WT development has been closely linked with epigenetic disturbance, and the phenomenon of loss of imprinting (LOI) was first demonstrated for the *IGF2* gene in WTs [6,7], and has subsequently been shown in a wide spectrum of other cancers [8]. In common with many other cancers, WTs also display two-hit epigenetic gene silencing, i.e., aberrant hypermethylation of tumor-suppressor gene 5′-CpG islands (CGI); examples include *RASSF1A* (in 42% of tumors) [9], *MCJ* (90%), *TNFRSF12* (65%) [10], *CASP8* (43%) and *MGMT* (30%) [11], and *SLIT2* (38%) [12].

We have also demonstrated WT-specific hypomethylation occurring at the *WT1* antisense regulatory region (*WT1* ARR) associated with LOI and the increased expression of a putative regulatory RNA, *WT1-AS* [13], and an alternative coding transcript, *AWT1* [14]. Hypomethylation occurs in a CCCTC binding

Abbreviations: AZA, 5-aza-2′-deoxycytidine; bp, base pair; CCSK, clear cell sarcoma of the kidney; CGI, CpG island; COBRA, combined bisulfite and restriction analysis; FK, fetal kidney; *GLIPR1/RTVP-1* gene, glioma pathogenesis–related 1/related to testis-specific, vespid, and pathogenesis proteins 1; LOI, loss of imprinting; NK, normal kidney; NR, nephrogenic rest; nt, nucleotides; RT-PCR, reverse transcriptase–polymerase chain reaction; WT, Wilms tumor

Address all correspondence to: Karim Malik, School of Medical Sciences, University of Bristol, University Walk, Bristol, Avon, UK. E-mail: k.t.a.malik@bristol.ac.uk

[1]These authors contributed equally.

Received 31 July 2007; Revised 4 October 2007; Accepted 5 October 2007.

DOI 10.1593/neo.07661

factor (CTCF)-binding region and is apparent in nephrogenic rests (NRs), suggesting an early impairment of methylation which would normally accompany kidney development, followed by extensive demethylation during expansion of the neoplastic rest and WT [15]. However, although genome-wide hypomethylation has long been known to be a common feature of all cancers [16], examples of genes that are activated by hypomethylation are very scarce compared with genes shown to be silenced by hypermethylation [17,18]. Examples of genes reportedly activated by hypomethylation include *MN/CA9* in renal cell carcinoma [19], *R-RAS* in gastric cancers [20], *PAX2* in endometrial carcinomas [21], and *SNCG* in a variety of adult cancers [22]. With recent genome analyses suggesting that methylation of CGIs in normal tissue may be more common than previously thought [23], many more genes may be deregulated by hypomethylation in cancer.

In screens for breast cancer–specific methylation changes using arrayed CGIs, a number of CGI tags were identified as being hypermethylated in breast cancer cell lines and tumor tissues. One such tag, referred to as HBC-2 [24], was found to correspond to the *WT1* ARR that we showed to undergo WT-specific hypomethylation [13]. To identify novel epigenetic changes in WTs, we assessed other CGI tags identified in the breast cancer studies and evaluated the methylation of the corresponding genomic loci. One tag (HBC-1) corresponded to an uncharacterized paralog of the glioma pathogenesis–related 1/related to testis-specific, vespid, and pathogenesis proteins 1 (*GLIPR1/RTVP-1*) gene, a proapoptotic p53 target gene [25]. Although it was originally identified as a gene overexpressed in gliomas where it has recently been reported to exert antiapoptotic functions [26,27], epigenetic silencing of *GLIPR1/RTVP-1* was demonstrated in prostate cancer, implicating it as a putative tumor-suppressor gene [28]. We were therefore prompted to evaluate its epigenetic status in WTs relative to normal fetal and pediatric kidney samples. We present data showing that, contrary to the hypermethylation evident in prostate cancers, *GLIPR1/RTVP-1* hypomethylation is prevalent in a high percentage of WTs. High expression of *GLIPR1/RTVP-1* is frequently observed in conjunction with hypomethylation. Hypomethylation is also apparent in WT precursor lesions, suggesting it as an early contributory event in Wilms tumorigenesis. Our data suggest that gene activation accompanying hypomethylation of non-imprinted genes is a previously uncharacterized form of epigenetic disruption prevalent in WTs.

Materials and Methods

Patient Samples

All tissues were acquired with appropriate ethical approval as snap frozen samples from the Bristol Children's Hospital and the University of Heidelberg Children's Hospital. WT tissues ranged from stage I to stage V and were obtained along with adjacent histologically normal kidney (NK) and, where available, NRs. Fetal kidney (FK) samples were from 19 to 31 weeks of gestation. A clear cell sarcoma of the kidney (CCSK) was also obtained along with adjacent histologically normal kidney. Details of clinical samples are given in Table 1. Extraction of total cellular RNA was performed as previously described [29].

DNA were evaluated for loss of heterozygosity using microsatellite markers D12S1052 and D12S869 on chromosome 12q21. No gains or losses were apparent in informative sam-

Table 1. Summary of Clinical and Molecular Features of Wilms Tumors Analyzed.

WT	Sex	Tumor/Age at Diagnosis (months)	Stage/Histology	Outcome	*WT1* Mutation Details	11p13 LOH	11p15 LOH	16q LOH
8	M	UL/67	III/tr, fh	A	N	LOH	LOH	HT
24	M	UL/13	I/tr, s, fh	A	5-bp deletion in exon 7	LOH	LOH	HT
28	F	UL/19	I/b, fh	A	N	HT	LOH	HT
29	F	UL/9	II/b, e, fh	R 1991, D 1991	N	HT	HT	HT
48	F	UL/44	I/b, s, fh	A		HT	HT	HT
54	F	BL/19	V	A	5-bp insertion exon 1: GERMLINE	LOH	LOH	HT
56	F	UL/50	II/b, s	A		LOH	HT	LOH
57	F	UL/48	III	A		HT	HT	HT
61	F	UL/43	II	A		LOH	LOH	HT
62	F	BL/39	V/tr	R 1995, D 1996		HT	HT	LOH
63	F	UL/35	II/tr, fh	R 1996, A		LOH	LOH	LOH
65	F	BL/56	V/tr	R 1996, A		HT	HT	LOH(L) N(R)
69	F	UL/43	II/fh	A		HT	HT	HT
71	M	UL/47	IV	A		HT	HT	LOH
72	M	/105				HT	HT	HT
77	M	UL/29	II	A		LOH	LOH	HT
83	F	UL/6	III/e, fh	R 2000, A				
84	F	UL/120	IV/tr, fh	D 2000		HT	HT	LOH
85	M	UL/19	I/tr, fh	R 2001, A		HT	*ni*	HT
HD9	M	UL/30	IA/s	A	4 bp insertion exon 6	HT		HT
HD14	M	UL/12	I/s	A	7 bp deletion in exon 1b: GERMLINE	LOH		LOH
HD2	F	BL/15	V/s	A	26 bp deletion in exon 1b: GERMLINE	LOH		HT
HD1	F	BL/7	V/s	A	C–A transition in exon 7: GERMLINE	LOH		HT
HD13	F	UL/8	III/s	A	16-bp deletion in exon 7	LOH		
ANS2	M	UL/21	II/tr	A	1700-kb deletion	HEM		

F, female; *M*, male; *UL*, unilateral; *BL*, bilateral; *fh*, favorable histology; *tr*, triphasic; *b*, blastemal predominant; *e*, epithelial predominant; *s*, stromal predominant; *A*, alive; *R*, relapsed; *D*, died; *N*, no; *LOH*, loss of heterozygosity; *HT*, heterozygous; *HEM*, constitutionally hemizygous; *blank spaces*, not done; *ni*, noninformative.

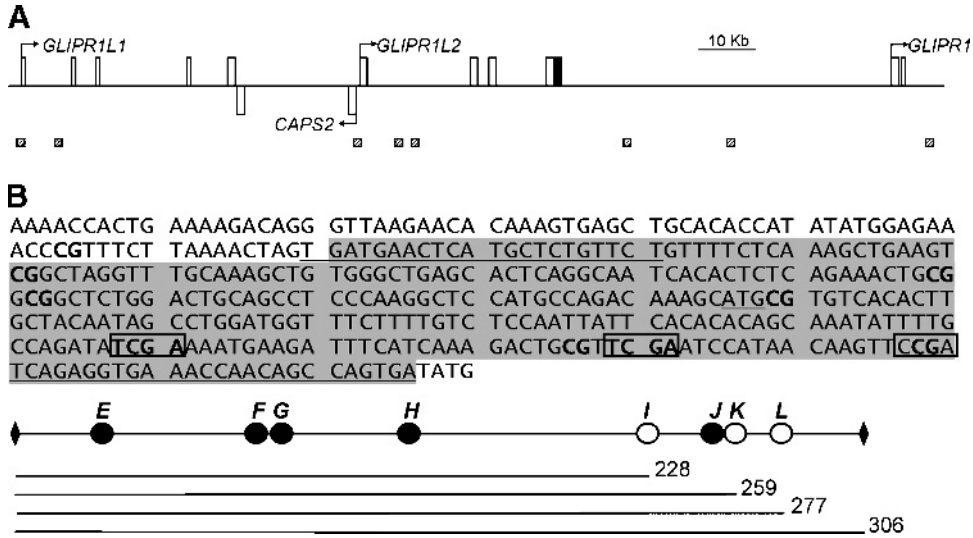

Figure 1. *The GLIPR1/RTVP-1 locus. (A) Schematic of the GLIPR1/RTVP-1 locus on chromosome 12q21. The top line shows the GLIPR1/RTVP-1 paralog cluster and CpG islands in this region (hatched boxes). (B) GLIPR1/RTVP-1 methylation analysis. The sequence of the GLIPR1/RTVP-1 upstream region is shown with CpGs in bold and exon 1 is shaded. Sites converted to* TaqI *sequences for COBRA are boxed, and the translational start site and COBRA primers are underlined. Restriction fragments generated by COBRA are shown below, with CpG sites analyzable by COBRA shown as open circles. Other CpGs are shown as closed circles, and all CpGs are labeled according to the previous analysis of prostate cancers [28].*

ples and, therefore, hypomethylation was distinguishable from allele loss.

Methylation Analyses

The HBC-1 sequence (see Figure 1) was analyzed using BLAST (www.ncbi.nlm.nih.co.uk/BLAST) and was found to align with the 5′-end of the *GLIPR1L1* gene, close to the *GLIPR1/RTVP-1* gene on chromosome 12q21 (see Figure 1*A*). For combined bisulfite and restriction analysis (COBRA) [30], genomic DNA were converted using the EZ DNA Methylation-Gold conversion kit (Zymo Research, Orange, CA) according to the manufacturer's instructions. CpGenome universally methylated DNA (Chemicon, Billerica, MA) was used as a positive control for COBRA assays and the following primer and digest combinations were used.

Gene	Primers	Annealing Temperature (°C)	Digest
GLIPR1	Left: TGATGAATTTAT-GTTTTGTTTTGTTTT Right: CACTAACTATTA-ATTTCACCTCTAATC	55	*Taq*I
GLIPR1L1	Left: TTTGGGATGGTT-GAAATTTTTTTTAT Right: TTAAAAACCCA-ACCCTATTCTTTCT	55	*Bsh1236*I/*Taq*I

Products were separated by agarose gel electrophoresis and band intensities were quantified using ImageJ software (http:rsb.info.nih.gov/ij/). Bisulfite sequencing used the COBRA primers and Hotstart plus *Taq* (Qiagen, Crawley, UK). Polymerase chain reaction (PCR) products were cloned into pGEM– T Easy (Promega, Southampton, UK) or TOPO TA Kit (Invitrogen, Paisley, UK) and positive clones were sequenced.

To generate a larger probe for *GLIPR1L1* by Southern blot analysis, the HBC-1 tag was used to screen a genomic library as described previously [31]. A plasmid subclone designated pλBE1.4 was generated from a positive phage clone and its insert was excised and radiolabeled for Southern blot analysis with genomic DNA digested with *Sac*II, *Eco*RI, and *Bam*HI. Experimental conditions were as previously described [13].

Reverse Transcriptase–Polymerase Chain Reaction (RT-PCR) Analysis

Total RNA (1 μg) was reverse-transcribed with oligo(dT)$_{20}$ at 60°C for 60 minutes using the ThermoScript RT-PCR System (Invitrogen) according to the manufacturer's instructions. RNA complementary to the cDNA was removed by incubating with 2 U RNaseH at 37°C for 20 minutes. cDNA was amplified using 5 μl of a 1:10 dilution of the reverse transcribed cDNA in a 25-μl PCR reaction containing 0.5 U *SuperTaq* (HT Biotechnology, Cambridge, UK), 0.2 mM each deoxyribonucleotide triphosphate (Sigma, Poole, UK) and 0.3 μM forward and reverse primers. For expression analyses, the following primers were used: *GLIPR1*, forward primer (5′–AGGCTCCATGCCAGACAAAGCATG–3′) and reverse primer (5′–CCTGAATTGTATTAGTCCAAAAGAAC–3′); *GLIPR1L1*, forward primer (5′–CTTTATAGACAACTGACTCGAAGC–3′) and reverse primer (5′–ACCTAATTTCCGACAGACGACTTCCA–3′); and *HPRT1*, forward primer (5′–CTTGCTGGTGAAAAGGACCCC–3′) and reverse primer (5′–GTCAAGGGCATATCCTACAAC–3′). Thermal cycling consisted of an initial denaturation step of 94°C for 4 minutes and was followed by 35 cycles with denaturation at 94°C for 30 seconds, annealing at 57°C for 30 seconds, and elongation at 72°C for 1 minute and 30 seconds. RT-PCR products were analyzed on a 1% agarose gel. For *GLIPR1L1*, gels were alkali-blotted onto Hybond-N$^+$ membrane and hybridized with ^{32}P-labeled cDNA probes.

Comparative Quantitative Real-Time PCR

Real-time PCR was performed using the Stratagene MX3000P QPCR System (La Jolla, CA) along with the Platinum SYBR green qPCR SuperMix-UDG (Invitrogen). Reactions volumes of 20 μl contained 10 μl of Platinum SYBR green qPCR SuperMix-UDG (Invitrogen, Paisley, UK), 50 nM ROX reference dye, 0.2 μM forward primer, 0.2 μM reverse primer, and 0.5 μl of cDNA template. Primers were: *GLIPR1*, forward primer (5′–GCGTTCGAATCCATAACAAGTTCC–3′) and reverse primer (5′–GGTGGCTTCAGCCGTGTATTATGTG–3′); *GLIPR1L1*, forward primer (5′–AATCCCATCCATCACTGACCCACA–3′) and reverse primer (5′–GCCCATGCTTTAGCCATCTTTGCT–3′); and *MCJ*, forward primer (5′–ACCAGCAGGGACTGGTAAGAAGTT–3′) and reverse primer (5′–TTCCAGATCCGAAATGCGTAGCGA–3′). Thermal cycling consisted of an initial incubation step of 50°C for 2 minutes and then a denaturation step of 95°C for 10 minutes. This was followed by 40 cycles of denaturation at 95°C for 15 seconds, annealing at 55°C for 30 seconds, and elongation at 72°C for 30 seconds. A final dissociation curve consisting of denaturation at 95°C for 1 minute, annealing at 55°C for 30 seconds, and elongation at 95°C for 30 seconds was used to identify a single correctly sized product. Gene expression was quantified by comparative C_t method, normalizing values to the housekeeping gene *TBP* or *GAPDH* and relative to a calibrator. Expression analysis for *TBP* was performed using forward primer (5′–GCCCGAAACGCCGAATAT–3′) and reverse primer (5′–CCGTGGTTCGTGGCTCTCT–3′) and for *GAPDH* it was performed using forward primer (5′–GTTCGACAGTCAGCCGCATC–3′) and reverse primer (5′–GGAATTTGCCATGGGTGGA–3′). To ensure experimental accuracy, all reactions were performed in duplicate.

Immunohistochemistry

Formalin-fixed, paraffin-embedded sections for FK and WT were sectioned at 6 μm on poly-L-lysine-coated slides. Immunostaining was carried out as previously reported [28] with the following modifications. Briefly, sections were rehydrated and blocked for endogenous peroxidase activity in 3% H_2O_2 in methanol. Following microwave antigen retrieval using citrate buffer, samples were blocked with 5% normal goat serum. An additional avidin/biotin blocking step was used to eliminate further endogenous biotin (Dako, Ely, UK). RTVP-1 primary antibody (a kind gift from Dr. T. Thompson, Baylor College of Medicine, TX) was diluted 1 in 2000 in phosphate-buffered saline and was incubated at room temperature for 4 hours. The secondary antibody was biotinylated goat anti-rabbit followed by horseradish peroxidase streptavidin (Dako). Visualization was with the DAB–substrate chromogen system (Dako).

5-Aza-2′-Deoxycytidine (AZA) Treatment

Anaplastic WT-derived cell lines 17.94 (Brown, unpublished observations) and WiT49 were treated 24 hours after seeding with 5 μM of the DNA methylation inhibitor AZA (Sigma). Treatment was repeated after a further 24-hour period, and again 48 hours after that. Cells were harvested after a final 24-hour incubation period.

Results

Hypomethylation of GLIPR1/RTVP-1 in WTs

The CGI tag, HBC-1, which undergoes tumor-specific hypermethylation in breast tumors [24], was found to correspond to the 5′-end of the *GLIPR1L1* gene. Methylation changes for this gene are described briefly below, but as nothing is known of *GLIPR1L1* function, and expression of this gene is low or absent in renal samples, it was not focused on. The *GLIPR1L1* gene is located in a paralog cluster on chromosome 12q21 (see Figure 1*A*) [32], which includes *GLIPR1L2* and *GLIPR1/RTVP-1*. As GLIPR1/RTVP-1 has been reported to have pro- and antiapoptotic activities [25,27], and the gene was silenced by hypermethylation in cancer [28], it was analyzed in detail.

We assessed methylation of the *GLIPR1/RTVP-1* gene in WTs using COBRA across CpGs shown to affect expression (sites I, K, and L according to Ren et al. [28]) (see Figure 1*B*). Whereas matched FKs (n = 3) and NKs (n = 17) exhibited considerable methylation of the *GLIPR1/RTVP-1* gene 5′-region, 21/24 WTs (87.5%) displayed extensive hypomethylation (see Figure 2*A*). One of the three FK samples assayed is shown, and one of the three WTs without hypomethylation (sample 61). Triphasic WTs, blastemal-rich WTs, and stromal predominant WTs (see Table 1) were all represented in the analysis and showed similar hypomethylation. We also observed a similar pattern in CCSK (sample 23). As COBRA encompasses only three CpG dinucleotides, we further assessed methylation changes using bisulfite sequencing. This confirmed that methylation was widespread in FK and NK at CpGs F–L (see Figure 1*B*), but virtually absent in WT (see Figure 2*B*).

Overexpression of GLIPR1/RTVP-1 in WTs

We analyzed 5 FK RNA, 18 NK RNA, and 24 WTs for *GLIPR1/RTVP-1* transcripts by quantitative RT-PCR, and representative results are shown in Figure 3*A*. Six NK samples (five fetal and one pediatric kidney) are shown on the left of the histogram, followed by six matched NK/WT pairs, and six WTs with characterized *WT1* mutations on the right [33]. Of the latter ANS2 had triphasic histology and the remainder were stromal predominant WTs (see Table 1). Five of the six tumors with matched NK showed *GLIPR1/RTVP-1* expression levels elevated 17- to 150-fold relative to 19-week-old FK, and the stromal predominant WTs showed 11- to 40-fold increases. Interestingly, tumor 62, despite exhibiting clear hypomethylation (see Figure 2*A*), expressed approximately 80% less *GLIPR1/RTVP-1* than the matched NK, the only tumor to show this pattern. This tumor is an anaplastic WT with a p53 mutation, and the lowered *GLIPR1/RTVP-1* expression in this sample is consistent with p53 being an activator of the *GLIPR1/RTVP-1* gene transcription [25]. Of 16 WTs where adjacent NK was also assessed, this was the only sample with

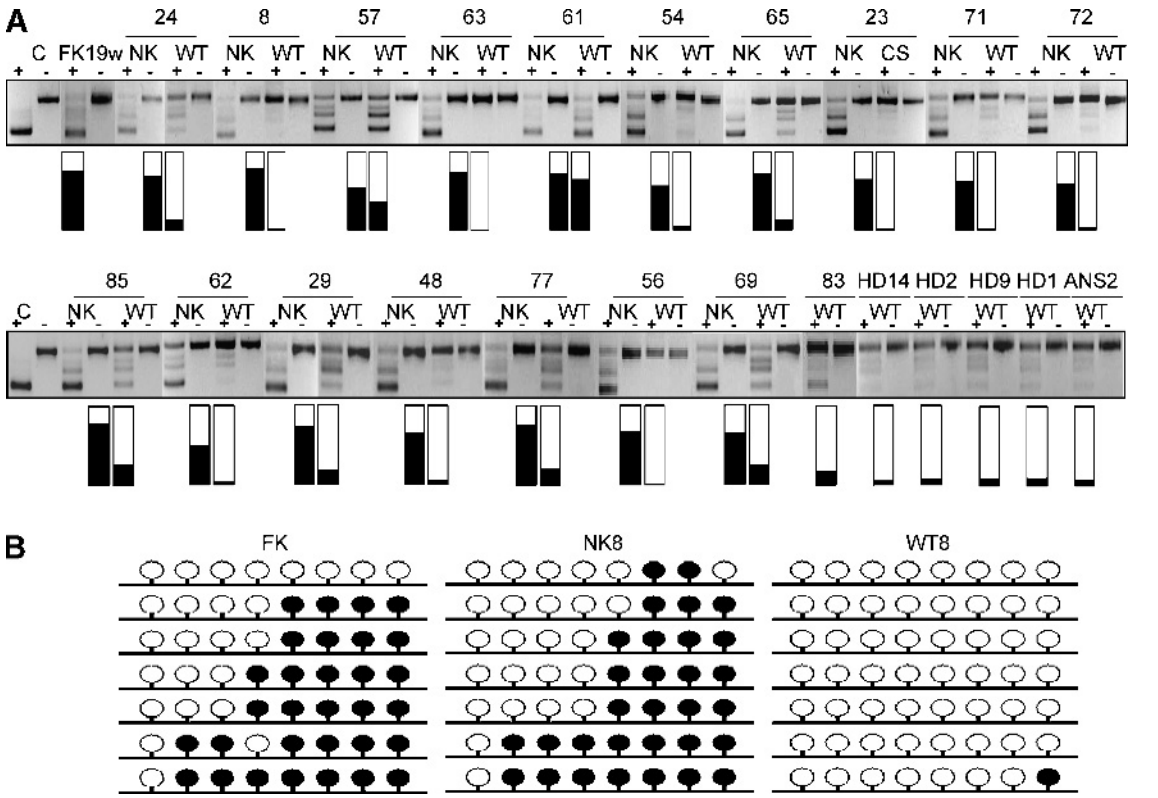

Figure 2. *Methylation analysis of GLIPR1/RTVP-1. (A) COBRA of kidneys and WTs.* FK*, fetal kidney;* NK*, normal kidney;* CS*, clear cell sarcoma of the kidney; C, control methylated DNA; (−), undigested; (+), digested. Densitometric analysis of methylation is shown as a histogram, where hypomethylated bands are expressed as a percentage of all bands, black fill indicating percentage methylation, and no fill indicating hypomethylation. (B) Bisulfite sequencing of kidney and tumor DNA. Filled lollipops represent methylated CpG dinucleotides and open lollipops represent unmethylated CpGs.*

reduced expression in the tumor. Of the remainder, 13/16 WTs had higher expression than NKs and 2 had equivalent levels. The CCSK displaying hypomethylation (sample 23; see Figure 2*A*) did not show marked overexpression compared to its matched NK (2.7-fold *vs* 4.1-fold). A plot of all kidney and WT samples analyzed is shown in Figure 3*B* and median expression levels for the three sample sets were 4.8 (FKs), 3.5 (NKs), and 21.9 (WTs). Sixteen of 24 WTs expressed *GLIPR1/RTVP-1* transcripts levels higher than the FK median. As previously shown [28], demethylation induced by treating cultured cells with AZA was found to increase *GLIPR1/RTVP-1* expression (Figure 3*C*).

Wilms tumors arise during embryonic kidney development and it is therefore imperative to evaluate molecular changes in WTs relative to FK. Expression of GLIPR1/RTVP-1 protein was assessed in these tissues using an anti–GLIPR1/RTVP-1 antibody previously used in analysis of prostate cancers [28]. Immunohistochemical staining of FK sections demonstrated nuclear expression of GLIPR1/RTVP-1 in epithelial cells of the primitive glomeruli and fainter expression in the blastema at the kidney edge, together with weak cytoplasmic staining in primitive tubules (see Figure 4). In a triphasic WT, GLIPR1/RTVP-1 was strongly expressed in blastemal cells, mainly in the cytoplasm. Staining in epithelial and stromal elements can be observed but was weaker or absent compared to the blastemal cells. Crucially, the tumor blastemal cells clearly expressed higher GLIPR1/RTVP-1 than the FK blastemal cells. Together with the methylation analysis, our RNA and protein expression data strongly suggests that *GLIPR1/RTVP-1* is induced by hypomethylation in WTs.

Hypomethylation Is an Early Event in Wilms Tumorigenesis

The preceding analyses strongly suggests that hypomethylation of specific genes in WTs can lead to their overexpression. However, it is uncertain whether such changes are a cause or consequence of tumor development. We therefore assessed the methylation status of *GLIPR1/RTVP-1* in WT precursor lesions and NRs. Figure 5 shows COBRA of a NK, WT, and NR set (patient 65), together with a second rest (patient 62). Both left and right tumors from patient 65 showed hypomethylation, and the NR showed partial hypomethylation (see Figure 5, *A* and *B*). A second NR from a different patient (62) showed comparable methylation to the patient 65 rest. These results are indicative of an early progressive decrease in gene-specific methylation during Wilms tumorigenesis or an expansion of cells with *GLIPR1/RTVP-1* hypomethylation.

GLIPR1/RTVP-1 Methylation Changes Are Specific and Not Regional

We used the HBC-1 tag to subclone a single-copy probe spanning the *GLIPR1L1* 5′-end to assess DNA methylation at a region proximal to *GLIPR1/RTVP-1* (see Figure 6*A*). As shown in Figure 6*C*, two major bands were apparent in

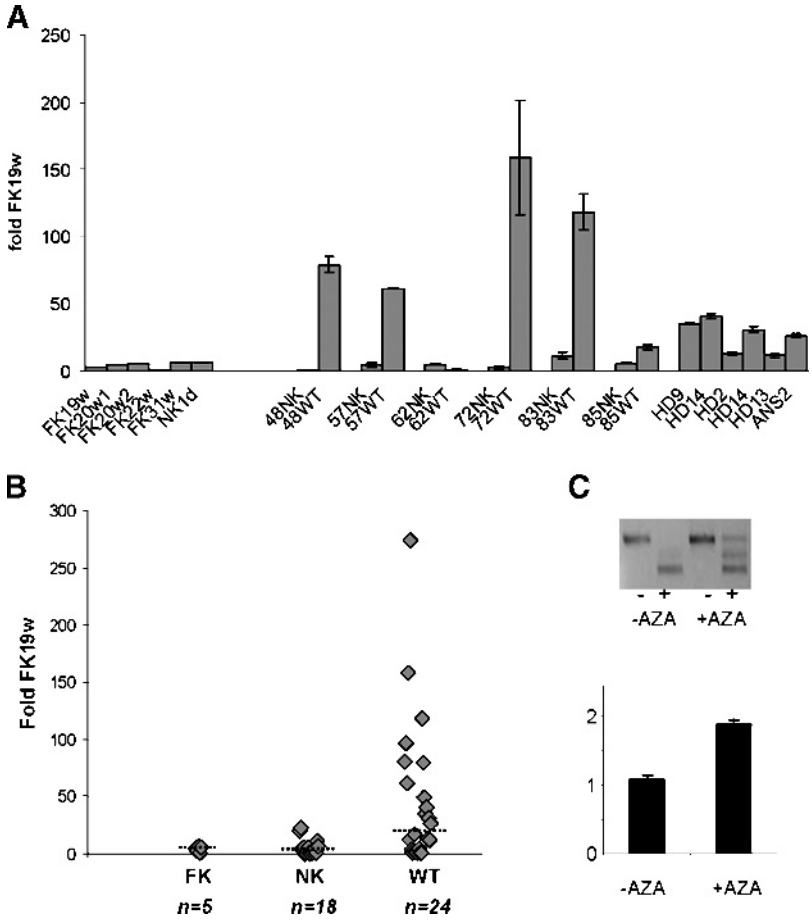

Figure 3. *Expression analyses of GLIPR1/RTVP-1. (A) Histogram showing* GLIPR1/RTVP-1 *mRNA expression in selected Wilms tumors relative to FK samples and matched NKs. Values are expressed as fold changes relative to a 19-week-old FK. (B) Scatter plot of quantitative RT-PCR analysis of control and tumor samples. The median value for each sample type is shown by the dashed line. (C) Correlation of AZA-induced methylation changes with altered gene expression. Histograms show relative changes in transcript levels and the panel above confirms demethylation by COBRA analysis: (−), undigested; (+), digested.*

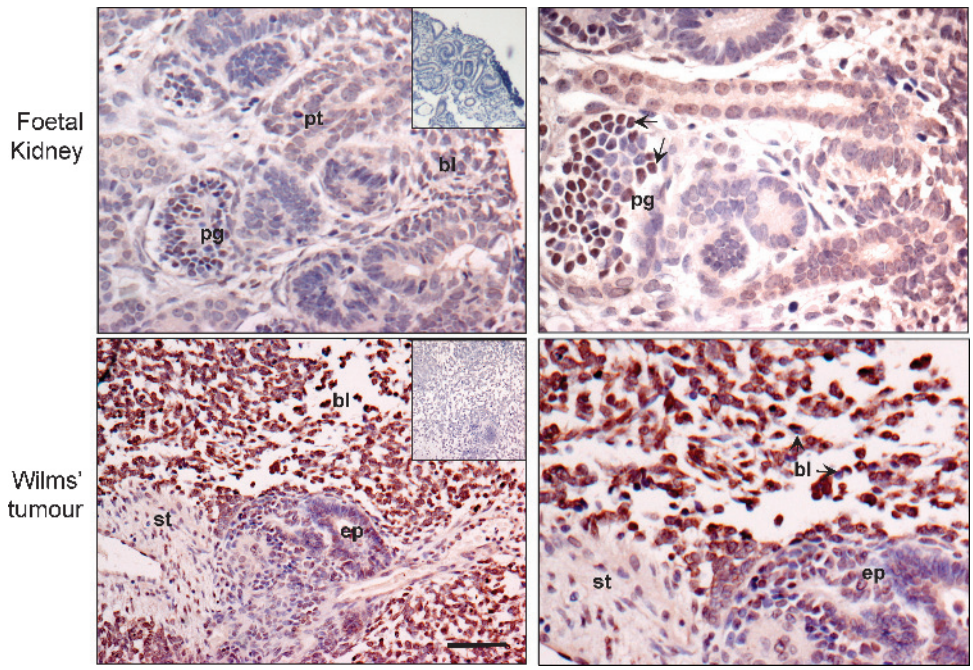

Figure 4. *Immunohistochemical analysis of* GLIPR1/RTVP-1 *protein expression. A 16-week-old FK and a triphasic WT are shown at low (left) and high magnification (right), with negative controls shown in the insets.* bl, *blastema;* ep, *epithelial cells;* pg, *primitive glomerulus;* pt, *primitive tubules;* st, *stroma. Nuclear staining in epithelial cells in FK and cytoplasmic staining in WT blastemal cells is arrowed in high-magnification pictures.*

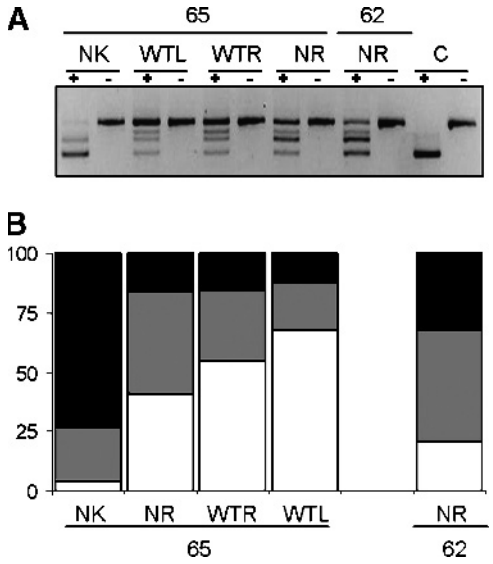

Figure 5. *Hypomethylation in NRs and bilateral Wilms tumor. (A) GLIPR1 COBRA of matched DNA from patient 65 and an additional NR from patient 62.* WTL*, left Wilms tumor;* WTR*, right Wilms tumor;* NR*, nephrogenic rest. (B) Percentage histogram of densitometric estimation of methylation (black), partial hypomethylation (gray), and complete hypomethylation (white).*

normal tissue DNA, corresponding in size to fragments digested (975 bp) and undigested (1410 bp) at the *Sac*II site within *GLIPR1L1* exon 1. Figure 6*C* (*top panel*) shows that 7/15 WTs examined had hypomethylation relative to the apparent differential methylation observed with normal DNA. A further 3/15 WTs showed no changes relative to their adjacent NK (patients 83, 86, and 69) and 5/15 of patient samples analyzed displayed apparent hypermethylation of *GLIPR1L1*. The Southern blot analysis of normal tissues and WTs representing hyper- and hypomethylated subsets was confirmed by bisulfite sequencing (see Figure 6*D*). Methylation in normal tissues was highly restricted in the region of the *Sac*II site and reflected the pattern of differential methylation observed by Southern blot analysis. One of the panel of tumors showing hypomethylation in Figure 6*C*, WT72, showed virtually no methylation, whereas bisulfite sequencing of WT81 was in accord with Southern blot data, displaying increased methylation relative to normal tissues. Thus, in contrast to *GLIPR1/RTVP-1*, *GLIPR1L1* appeared consistently and differentially methylated in normal tissues and displayed very variable methylation patterns in WTs. Importantly, the epigenetic heterogeneity at this locus suggests that the high frequency of hypomethylation observed for *GLIPR1/RTVP-1* is not merely a reflection of locus or cell type–specific methylation changes, as many samples that show hypomethylation at *GLIPR1/RTVP-1* do not show hypomethylation at *GLIPR1L1* (compare samples 24, 61, 63, 69, 83, and 85 in Figures 2*A* and 6*C*). We assessed *GLIPR1L1* transcript levels in kidney and WT samples and, although expression was too low to detect by RT-PCR, very low levels could be detected after Southern blot analysis and hybridization with radioactive probes in six

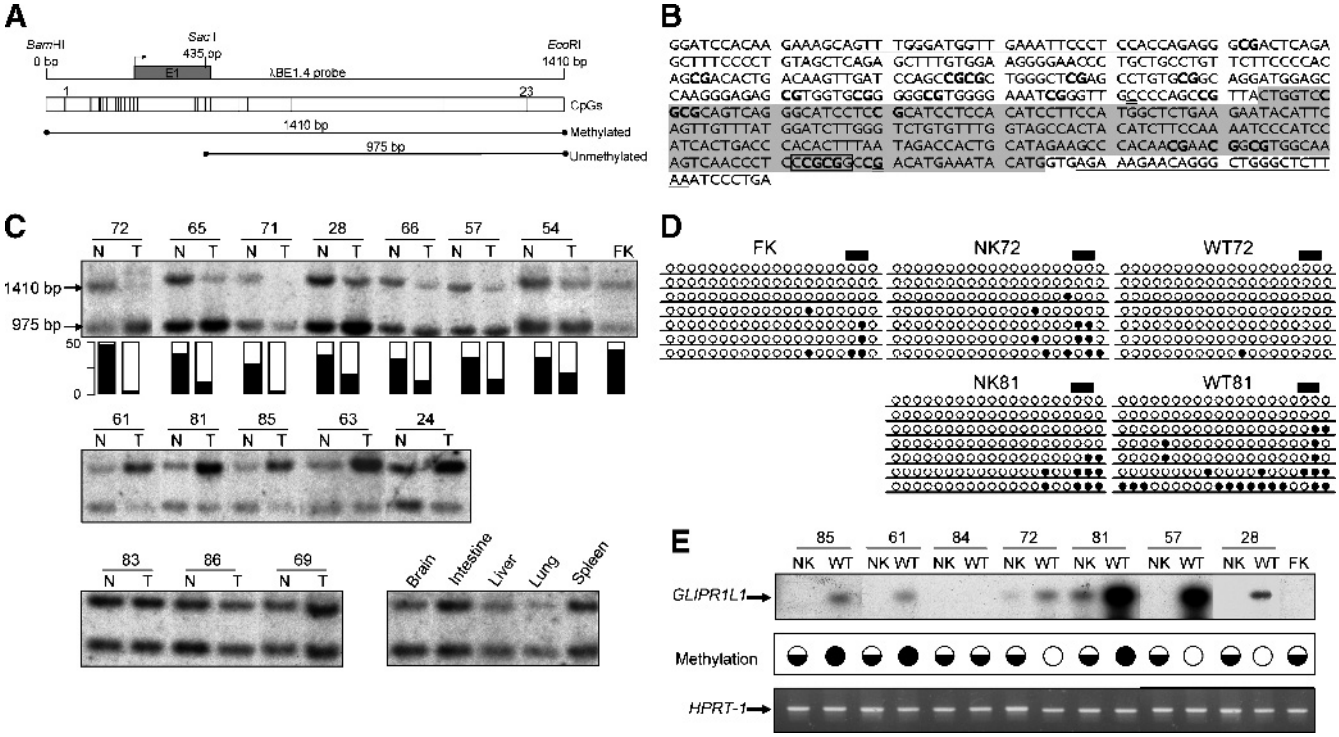

Figure 6. *Methylation and expression analysis of GLIPR1L1. (A) The methylation assay contingent on* Sac*II methylation status is shown with possible fragments and CpG distribution. (B) Sequence of the GLIPR1L1 upstream region. The sequence of the HBC-1 tag is between the double-underlined bases, CpGs are shown in bold, and exon 1 is shaded. The* Sac*II site is boxed, and primer regions for COBRA are underlined. (C) Southern blots showing WTs with hypomethylation (top panel) and hypermethylation (middle panel). Densitometric quantification for hypomethylation is shown as a histogram, where 50% denotes equal intensities of 1410- and 975-bp bands and 0% denotes complete absence of the 1410-bp band. The bottom panel shows WTs and fetal DNA with no change. (D) Bisulfite sequencing of kidney and tumor DNA. Filled lollipops represent methylated CpG dinucleotides and open lollipops represent unmethylated CpGs. The black bars mark the two CpG residues within the* Sac*II site used in Southern blot analysis. (E)* GLIPR1L1 *RT-PCR analysis shown with methylation summary for assayed samples and* HPRT-1 *as housekeeping control.*

patient samples (see Figure 6*E*). All other samples were negative. Although WTs appear to express higher levels of *GLIPR1L1* than kidney controls, the expression did not correlate with methylation status, as samples with tumor hypermethylation (61, 81, and 85) and hypomethylation (28, 57, and 72) had detectable *GLIPR1L1*.

Discussion

The analysis of tumor-suppressor gene silencing in cancer cells is a major focus of contemporary cancer research. However, there is increasing evidence that gene activation associated with hypomethylation is involved in cancer. Examples include *PAX2* activation in endometrial carcinomas [21] and *SNCG* activation in a wide variety of human cancers [22]. In this report, we show for the first time that hypomethylation-associated gene activation of nonimprinted genes is found in WT, with the *GLIPR1/RTVP-1* gene displaying deregulated expression in tumors relative to normal fetal and pediatric kidney. Furthermore, we demonstrate that altered methylation is detectable in WT precursor lesions, suggesting that these changes occur early and may contribute to tumorigenesis.

Our methylation analysis of *GLIPR1/RTVP-1* reveals remarkably frequent tumor-specific hypomethylation of the gene, apparent in 87.5% of WTs ($n = 24$). By way of comparison, *R-RAS* analysis showed partial hypomethylation in 3/5 primary gastric [20]. Also, whereas a large study of the *SNCG* in adult cancers demonstrated hypomethylation of this gene in all tumors ($n = 20$ per tumor), hypomethylation was also observed in 30% of normal adjacent tissue [22], in contrast to our findings of highly tumor-specific hypomethylation. *GLIPR1/RTVP-1* has already been shown to be epigenetically altered (hypermethylated) in prostate cancer, and it will clearly be of great interest to evaluate its epigenetic status in other cancers.

GLIPR1/RTVP-1 has been shown to be a p53-regulated proapoptotic tumor-suppressor gene undergoing epigenetic silencing in prostate cancer [25,28]. However, in glioma cells, *GLIPR1/RTVP-1* expression is high [26,27]. Quantitative mRNA analysis revealed that *GLIPR1/RTVP-1* levels were approximately 3-fold higher in low-grade astrocytomas compared to normal brain, with glioblastomas being 8-fold higher. Strikingly, our expression analysis of WTs shows that over half express mRNA levels in excess of 20-fold relative to FK, with some even exceeding 100-fold. In all, 16 WTs showed elevated expression levels, whereas 8 did not; of the latter, 2 displayed no hypomethylation, and 1 tumor had a p53 mutation. Hence, for 5 of 24 tumors, there was no direct correlation between methylation/genetic factors and *GLIPR1/RTVP-1* expression. Similar results have been observed for other genes undergoing hypomethylation such as *SNCG* [22], where approximately 30% of tumors did not show a methylation/expression correlation. This is likely attributable to the absence or alteration of other cellular proteins which may be necessary for high-level expression of *GLIPR1/RTVP-1*. Concomitant requirement for hypomethylation and upregulation of the transcription factor early growth response-1 has been reported for heparanase gene overexpression in prostate [34] and bladder cancers [35].

In glioma cells, the GLIPR1/RTVP-1 protein positively regulates growth, survival, and invasion. GLIPR1/RTVP-1 overexpression results in elevated Bcl2, leading to an antiapoptotic effect, and increases the activity of matrix metalloproteinase-2, thereby positively regulating the invasive potential of glioma cells [27]. We also note that the *scl-1* gene in *Caenorhabditis elegans*, which is homologous to *GLIPR1/RTVP-1*, has been shown to encode a regulator of longevity and stress resistance [36]. Our methylation analysis of *GLIPR1/RTVP-1* revealed tumor-specific hypomethylation and overexpression relative to FK and NK in WTs. Although the biologic roles of GLIPR1/RTVP-1 in WT cells remain to be elucidated, it is plausible that, as in the case of gliomas, GLIPR1/RTVP-1 exerts a proliferative, prosurvival influence.

Our recent study of epigenetic deregulation of *AWT1/WT1-AS* in WTs showed that LOI is an early event in Wilms tumorigenesis [15]. Hypomethylation of *GLIPR1/RTVP-1* is apparent in NRs and in left and right tumors where WT is bilateral. Although the progressive increase in hypomethylation seen in NRs might be considered to simply reflect an expansion of oncofetal cells, our previous work argues against this as methylation at the *WT1* ARR in NRs shows a general increase relative to FK [15]. Therefore, the early gene-specific hypomethylation reported for *GLIPR1/RTVP-1* may contribute to Wilms tumorigenesis, rather than merely accompanying tumorigenesis. This is supported by our immunohistochemical analysis showing that WT blastemal cells express very high levels of GLIPR1/RTVP-1 compared to FK blastemal cells. Overexpression of GLIPR1/RTVP-1 in WT may serve as a useful diagnostic marker, although therapeutic use may be complicated by GLIPR1/RTVP-1 expression seemingly required for NK development and function.

Our methylation analysis of *GLIPR1L1* further supports the contention that *GLIPR1/RTVP-1* methylation changes in WT are specific and not just regional. Our preliminary analysis also shows that the *GLIPR1L2* gene does not undergo epigenetic alterations in WT (data not shown). Although some methylation changes are observed at the *GLIPR1L1* gene, they are inconsistent and do not correlate with expression. Expressions of *GLIPR1L1* by Northern blot analysis (data not shown) and by quantitative RT-PCR [32] show that it is highly expressed in the testis with little or no expression in other tissues. This highly restricted expression pattern, together with the expression shown here in tumors, suggests that *GLIPR1L1* can be considered a cancer–testis gene. Cancer–testis proteins are only found in a minor subset of cells within a tumor and it has been suggested that they may serve as a marker for cancer stem cells [37]. Thus, although *GLIPR1L1* expression was very low in WT samples, it may yet be a valuable target for immunotherapy against cancer stem cells.

Finally, given that a recent analysis of the human genome suggests that methylation of non-CGI upstream regions is relatively common [23,38], our study underlines the need for extensive analysis of gene activation by hypomethylation and emphasizes an important caveat for cancer therapies using DNA methylation inhibitors, because these may inappropriately activate tumor-promoting genes.

Acknowledgements

The authors thank the Cancer and Leukaemia in Childhood Sargent Research Trust and the Children's Leukaemia Trust for financial support. We thank T. Thompson for the GLIPR1/RTVP-1 antibody, Adrian Charles for the microdissected nephrogenic rest samples and Z. Melegh for helpful comments.

References

[1] Hastie ND (1994). The genetics of Wilms' tumor — a case of disrupted development. *Annu Rev Genet* **28**, 523–558.

[2] Call KM, Glaser T, Ito CY, Buckler AJ, Pelletier J, Haber DA, Rose EA, Kral A, Yeger H, and Lewis WH (1990). Isolation and characterization of a zinc finger polypeptide gene at the human chromosome 11 Wilms' tumor locus. *Cell* **60**, 509–520.

[3] Gessler M, Poustka A, Cavenee W, Neve RL, Orkin SH, and Bruns GA (1990). Homozygous deletion in Wilms tumours of a zinc-finger gene identified by chromosome jumping. *Nature* **343**, 774–778.

[4] Rivera MN and Haber DA (2005). Wilms' tumour: connecting tumorigenesis and organ development in the kidney. *Nat Rev Cancer* **5**, 699–712.

[5] Rivera MN, Kim WJ, Wells J, Driscoll DR, Brannigan BW, Han M, Kim JC, Feinberg AP, Gerald WL, Vargas SO, et al. (2007). An X chromosome gene, *WTX*, is commonly inactivated in Wilms tumor. *Science* **315**, 642–645.

[6] Ogawa O, Eccles MR, Szeto J, McNoe LA, Yun K, Maw MA, Smith PJ, and Reeve AE (1993). Relaxation of insulin-like growth factor-II gene imprinting implicated in Wilms' tumour. *Nature* **362**, 749–751.

[7] Rainier S, Johnson LA, Dobry CJ, Ping AJ, Grundy PE, and Feinberg AP (1993). Relaxation of imprinted genes in human cancer. *Nature* **362**, 747–749.

[8] Feinberg AP (1999). Imprinting of a genomic domain of 11p15 and loss of imprinting in cancer: an introduction. *Cancer Res* **59**, 1743–1746.

[9] Harada K, Toyooka S, Maitra A, Maruyama R, Toyooka KO, Timmons CF, Tomlinson GE, Mastrangelo D, Hay RJ, Minna JD, et al. (2002). Aberrant promoter methylation and silencing of the *RASSF1A* gene in pediatric tumors and cell lines. *Oncogene* **21**, 4345–4349.

[10] Ehrlich M, Jiang G, Fiala E, Dome JS, Yu MC, Long TI, Youn B, Sohn OS, Widschwendter M, Tomlinson GE, et al. (2002). Hypomethylation and hypermethylation of DNA in Wilms tumors. *Oncogene* **21**, 6694–6702.

[11] Morris MR, Hesson LB, Wagner KJ, Morgan NV, Astuti D, Lees RD, Cooper WN, Lee JA, Gentle D, Macdonald F, et al. (2003). Multigene methylation analysis of Wilms' tumour and adult renal cell carcinoma. *Oncogene* **22**, 6794–6801.

[12] Astuti D, Da Silva NF, Dallol A, Gentle D, Martinsson T, Kogner P, Grundy R, Kishida T, Yao M, Latif F, et al. (2004). *SLIT2* promoter methylation analysis in neuroblastoma, Wilms' tumour and renal cell carcinoma. *Br J Cancer* **90**, 515–521.

[13] Malik K, Salpekar A, Hancock A, Moorwood K, Jackson S, Charles A, and Brown KW (2000). Identification of differential methylation of the *WT1* antisense regulatory region and relaxation of imprinting in Wilms' tumor. *Cancer Res* **60**, 2356–2360.

[14] Dallosso AR, Hancock AL, Brown KW, Williams AC, Jackson S, and Malik K (2004). Genomic imprinting at the *WT1* gene involves a novel coding transcript (*AWT1*) that shows deregulation in Wilms' tumours. *Hum Mol Genet* **13**, 405–415.

[15] Hancock AL, Brown KW, Moorwood K, Moon H, Holmgren C, Mardikar SH, Dallosso AR, Klenova E, Loukinov D, Ohlsson R, et al. (2007). A CTCF-binding silencer regulates the imprinted genes *AWT1* and *WT1-AS* and exhibits sequential epigenetic defects during Wilms' tumourigenesis. *Hum Mol Genet* **16**, 343–354.

[16] Feinberg AP and Vogelstein B (1983). Hypomethylation distinguishes genes of some human cancers from their normal counterparts. *Nature* **301**, 89–92.

[17] Ehrlich M (2002). DNA methylation in cancer: too much, but also too little. *Oncogene* **21**, 5400–5413.

[18] Esteller M (2007). Cancer epigenomics: DNA methylomes and histone–modification maps. *Nat Rev Genet* **8**, 286–298.

[19] Cho M, Uemura H, Kim SC, Kawada Y, Yoshida K, Hirao Y, Konishi N, Saga S, and Yoshikawa K (2001). Hypomethylation of the *MN/CA9* promoter and upregulated *MN/CA9* expression in human renal cell carcinoma. *Br J Cancer* **85**, 563–567.

[20] Nishigaki M, Aoyagi K, Danjoh I, Fukaya M, Yanagihara K, Sakamoto H, Yoshida T, and Sasaki H (2005). Discovery of aberrant expression of *R-RAS* by cancer-linked DNA hypomethylation in gastric cancer using microarrays. *Cancer Res* **65**, 2115–2124.

[21] Wu HJ, Chen YP, Liang J, Shi B, Wu G, Zhang Y, Wang D, Li RF, Yi X, Zhang H, et al. (2005). Hypomethylation-linked activation of *PAX2* mediates tamoxifen-stimulated endometrial carcinogenesis. *Nature* **438**, 981–987.

[22] Liu HY, Liu W, Wu YW, Zhou Y, Xue R, Luo C, Wang L, Zhao W, Jiang JD, and Liu JW (2005). Loss of epigenetic control of Synuclein-gamma gene as a molecular indicator of metastasis in a wide range of human cancers. *Cancer Res* **65**, 7635–7643.

[23] Strichman-Almashanu LZ, Lee RS, Onyango PO, Perlman E, Flam F, Frieman MB, and Feinberg AP (2002). A genome-wide screen for normally methylated human CpG islands that can identify novel imprinted genes. *Genome Res* **12**, 543–554.

[24] Huang THM, Laux DE, Hamlin BC, Tran P, Tran H, and Lubahn DB (1997). Identification of DNA methylation markers for human breast carcinomas using the methylation-sensitive restriction fingerprinting technique. *Cancer Res* **57**, 1030–1034.

[25] Ren CH, Li LK, Goltsov AA, Timme TL, Tahir SA, Wang JX, Garza L, Chinault AC, and Thompson TC (2002). *mRTVP-1*, a novel p53 target gene with proapoptotic activities. *Mol Cell Biol* **22**, 3345–3357.

[26] Murphy EV, Zhang Y, Zhu WJ, and Biggs J (1995). The human glioma pathogenesis–related protein is structurally related to plant pathogenesis–related proteins and its gene is expressed specifically in brain-tumors. *Gene* **159**, 131–135.

[27] Rosenzweig T, Ziv-Av A, Xiang CL, Lu W, Cazacu S, Taler D, Miller CG, Reich R, Shoshan Y, Anikster Y, et al. (2006). Related to testes-specific, vespid, and pathogenesis protein-1 (RTVP-1) is overexpressed in gliomas and regulates the growth, survival, and invasion of glioma cells. *Cancer Res* **66**, 4139–4148.

[28] Ren C, Li L, Yang G, Timme TL, Goltsov A, Ren C, Ji X, Addai J, Luo H, Ittmann MM, et al. (2004). RTVP-1, a tumor suppressor inactivated by methylation in prostate cancer. *Cancer Res* **64**, 969–976.

[29] Malik KTA, Wallace JI, Ivins SM, and Brown KW (1995). Identification of an antisense *WT1* promoter in intron 1: implications for *WT1* gene regulation. *Oncogene* **11**, 1589–1595.

[30] Xiong ZG and Laird PW (1997). COBRA: a sensitive and quantitative DNA methylation assay. *Nucleic Acids Res* **25**, 2532–2534.

[31] Malik KTA, Poirier V, Ivins SM, and Brown KW (1994). Autoregulation of the human *WT1* gene promoter. *FEBS Lett* **349**, 75–78.

[32] Ren CZ, Ren CH, Li LK, Goltsov AA, and Thompson TC (2006). Identification and characterization of RTVP1/GLIPR1–like genes, a novel p53 target gene cluster. *Genomics* **88**, 163–172.

[33] Schumacher V, Schneider S, Figge A, Wildhardt G, Harms D, Schmidt D, Weirich A, Ludwig R, and Royerpokora B (1997). Correlation of germ-line mutations and two-hit inactivation of the *WT1* gene with Wilms tumors of stromal-predominant histology. *Proc Natl Acad Sci USA* **94**, 3972–3977.

[34] Ogishima T, Shiina H, Breault JE, Tabatabai L, Bassett WW, Enokida H, Li LC, Kawakami T, Urakami S, Ribeiro-Filho LA, et al. (2005). Increased heparanase expression is caused by promoter hypomethylation and up-regulation of transcriptional factor early growth response-1 in human prostate cancer. *Clin Cancer Res* **11**, 1028–1036.

[35] Ogishima T, Shiina H, Breault JE, Terashima M, Honda S, Enokida H, Urakami S, Tokizane T, Kawakami T, Ribeiro LA, et al. (2005). Promoter CpG hypomethylation and transcription factor EGR1 hyperactivate heparanase expression in bladder cancer. *Oncogene* **24**, 6765–6772.

[36] Ookuma S, Fukuda M, and Nishida E (2003). Identification of a DAF-16 transcriptional target gene, *scl-1*, that regulates longevity and stress resistance in *Caenorhabditis elegans*. *Curr Biol* **13**, 427–431.

[37] Simpson AJG, Caballero OL, Jungbluth A, Chen YT, and Old LJ (2005). Cancer/testis antigens, gametogenesis and cancer. *Nat Rev Cancer* **5**, 615–625.

[38] Eckhardt F, Lewin J, Cortese R, Rakyan VK, Attwood J, Burger M, Burton J, Cox TV, Davies R, Down TA, et al. (2006). DNA methylation profiling of human chromosomes 6, 20 and 22. *Nat Genet* **38**, 1378–1385.